Lapai Journal of Science and Technology, Vol. 7, No. 1 (2021)

ANALYSIS OF FIRE OUTBREAK IN COUPLED ATMOSPHERIC-WILDFIRE

[*1]Zhiri, A. B., [1]Olayiwola, R. O., [1]Audu, K. J., [2]Adeloye, T. O. and [1]Gupa, M. I.

[1]Department of Mathematics Federal University of Technology, Minna, Nigeria.
[2]Department of Mathematics Nigeria Maritime University, Okerenkoko, Warri, Delta State, Nigeria

*Corresponding e-mail: a.zhiri@futminna.edu.ng

ABSTRACT

Forest fire outbreak has become alarming day by day as it is a common occurrence in most parts of the world and it cause a lot of havoc to biodiversity as well as to the local ecology. In this paper, a partial differential equations (PDE) governing wildland fire outbreak is presented. We obtained the approximate analytical solution of the model using perturbation method, direct integration and eigenfunction expansion technique, which clearly depicts the influence of the parameters involved in the system. The effect of change in parameters such as Radiation number, Peclet energy number, Peclet mass number, and Equilibrium wind velocity on oxygen concentration are shown graphically and discussed. The results obtained revealed that as Radiation number and Peclet energy number increases, oxygen concentration depreciates. While increasing Peclet mass number, and Equilibrium wind velocity enhanced oxygen concentration.

KEYWORDS: Eigenfunction expansion technique, Fire spread outbreak, fuel, wind, wind flow.

INTRODUCTION

Wind is arguably the most important weather and climate factor that influences the pattern and behaviour of a fire (Taylor *et al.,* 2004). There are three types of wind that are associated with wildfire: general winds resulting from atmospheric activity, local winds resulting from unequal heating of land and sea surfaces, and winds resulting from a fire's buoyancy (also called entrainment). Most wildfires move in one or more directions depending on the availability of fuels, wind direction, and topography. If fuels are discontinuous (e.g., as in deserts), then a fire may not spread successfully unless wind velocity and direction are sufficient to cause a fire to ''leap'' the gap between fuels (Randall *et al.,* 2009).

Air moves in response to pressure differences in earth's atmosphere and as a result of frictional effects near earth's surface. Wind affects fire occurrence and especially fire behaviour at the synoptic, regional, and microclimate scales. Winds associated with cold

fronts are also important to smoke dispersal from large fires (Freitas *et al.,* 2005). Meroney (2007) discusses the effects of wind flow in both the urban and forested fire spread environments. These wind flow also influence the distribution and transportation of pollutants and smoke within urban and wildland–urban interface settings. Potter (2002) developed a conceptual model of plume and fire dynamics. This model describes dynamics in three layers: surface, mixing, and stable. The interaction of a fire and its plume varies in these layers, and influential atmospheric variables may change between layers. He stated that presence of wind further complicates fire behaviour.

Mandel *et al.* (2018) studied Coupled atmosphere-wildland fire modelling with Weather Research and Forecasting (WRF) Fire. They described the coupled atmosphere-fire model WRF-Fire, as they did not support canopy fire, although canopy fire collocated with ground fire is contained in Coupled Atmospheric Wildland Fire Environment (CAWFE). In a coupled model, however, the feedback on the fire is from the wind that is influenced by the fire. Zhiri *et al.* (2020) worked on modelling fire spread behaviour in coupled atmospheric-forest fire using direct integration and eigenfunction expansion technique to obtained analytical solution and concluded that, an increase in activation energy number causes temperature to retard but oxygen concentration is enhanced.

Forest fire are often channel towards direction of the wind. The rates and completeness of combustion often differ as a function of gas phase in fire spread outbreak, which in turn influences the production of smoke. Perminov (2018) worked on mathematical modeling of wildland fires initiation and spread using a coupled atmospheric-forest fire setting. The method of finite volume is used to obtain discrete analogies. The boundary-value problem is solved numerically using the method of splitting according to physical processes. He estimated the amount of carbon dioxide and carbon monoxide emissions at crown forest fire spread.

In this regards, this paper extended the model investigated by Perminov (2018) and established an approximate analytical solutions that is capable of determining the influence of radiation number, peclet energy number, peclet mass number, and equilibrium wind velocity

particularly on the gas phase of fire outbreak in coupled atmospheric-wildfire. This will be achieved using perturbation method, direct integration and eigenfunction expansion technique.

MODEL FORMULATIONS

Following Perminov (2018) we consider a wildfire model. We assume that the gas phase consist of only oxygen, there is thermal equilibrium between the gas and solid, pressure and wind velocity of the forest canopy are constant, ash is neglected and the forest environment consist of five-phase porous medium which are dry organic substance (Matter), water in liquid state (Moisture), solid pyrolysis product (coke) ash and gas phase. Under these assumptions, the equations that describe wildland fire propagation are:

Volume fraction of dry organic substance

$$\frac{\partial \varphi_s}{\partial t} = -k_1 \varphi_s e^{-\frac{E_1}{RT}} \tag{1}$$

Volume fraction of moisture

$$\frac{\partial \varphi_m}{\partial t} = -k_2 \varphi_m T^{\frac{1}{2}} e^{-\frac{E_2}{RT}} \tag{2}$$

Volume fraction of coke

$$\rho_c \frac{\partial \varphi_c}{\partial t} = \alpha_c k_1 \rho_s \varphi_s e^{-\frac{E_1}{RT}} - \frac{M_c}{M_1} k_3 S_\sigma \rho_g \varphi_c C_{ox} e^{-\frac{E_3}{RT}} \tag{3}$$

Mass concentration of oxygen

$$\left.\begin{aligned} \rho_g \left(\frac{\partial C_{ox}}{\partial t} + v \frac{\partial C_{ox}}{\partial x} \right) = \frac{\partial}{\partial x} \left(\rho_g D_T \frac{\partial C_{ox}}{\partial x} \right) - \frac{\alpha}{C_{pg} \Delta h} \left(C_{ox} - C_{ox_\infty} \right) - \\ \left(1-\alpha_c\right) k_1 \rho_s \varphi_s C_{ox} e^{-\frac{E_1}{RT}} - k_2 \rho_m T^{\frac{1}{2}} \varphi_m C_{ox} e^{\frac{-E_2}{RT}} - k_3 S_\sigma \rho_g \left(1 + \frac{M_c}{M_1} C_{ox} \right) \varphi_c C_{ox} e^{\frac{-E_3}{RT}} \end{aligned}\right\} \tag{4}$$

Energy balance equation

$$\left.\begin{aligned} \left(\phi \rho_g C_{pg} + \left(1-\phi\right) \sum_{i=1}^{s+m+c} \rho_i C_{pi} \varphi_i \right) \frac{\partial T}{\partial t} + \rho_g C_{pg} v \frac{\partial T}{\partial x} = \frac{\partial}{\partial x} \left(\lambda_T \frac{\partial T}{\partial x} \right) - \frac{\alpha}{\Delta h} \left(T - T_\infty \right) \\ -4 K_R \sigma T^4 - k_2 \rho_m q_2 T^{\frac{1}{2}} \varphi_m e^{\frac{-E_2}{RT}} + k_3 S_\sigma \rho_g q_3 \varphi_c C_{ox} e^{\frac{-E_3}{RT}} \end{aligned}\right\} \tag{5}$$

Satisfying the initial and boundary conditions:

$$\left.\begin{array}{l}\varphi_s(x,0)=\varphi_{so},\ \varphi_m(x,0)=\varphi_{mo},\ \varphi_c(x,0)=\varphi_{co},\ C_{ox}(x,0)=C_{ox_o},\ C_{ox}(0,t)=C_{ox_\infty}\\ C_{ox}(\mathrm{L},t)=C_{ox_\infty},\ T(x,0)=T_o,\ T(0,t)=T_\infty,\ T(\mathrm{L},t)=T_\infty\end{array}\right\} \quad (6)$$

where;

φ_s is the volume fraction of dry organic substance, φ_m is the volume fraction of moisture, φ_c is the volume fraction of coke, C_{ox} is the concentration of oxygen, T is the temperature (in Kelvin), t is the time, x is a coordinate in the system of coordinates connected with the centre of an initial fire (distance), T_∞ is the unperturbed ambient temperature, $k_j, j=1,2,3$ are the pre- exponential factors of chemical reactions, $E_j, j=1,2,3$ are the activation energy of chemical reactions, C is the concentration, R is the universal gas constant, S_σ is the specific surface of the condensed product of pyrolysis (coke), v is the equilibrium wind velocity vector, U is the reference velocity, λ_T is the turbulent thermal conductivity, C_{ox_∞} is the unperturbed density of concentration of oxygen, $P_i, i=(s,m,c)$ is the i^{-th} phase density, that is ρ_s is the density of dry organic substance, ρ_m is the density of moisture, ρ_c is the density of coke, ρ_g is the density of gas phase (a mix of gases), Δh is the crown height, M_c is the molecular mass of carbon, M_1 is the mass of combustible forest material (CFM), C_{pg} is the thermal capacity of a gas phase, $q_j, j=2,3$ defines heat effects of processes of evaporation of burning, D_T is the diffusion coefficient, α is the coefficient of heat exchange between the atmosphere and a forest canopy, α_c is the coke number of combustible forest material (CFM), σ is the Stefan-BoltzMann constant, K_R is the integrated absorptance, $C_{p_i}, i=(s,m,c)$ is the i^{-th} phase of thermal capacity, s is the dry organic substance, m is the moisture, c is the coke, ox is the oxygen (O_2).

METHODS OF SOLUTION

Non-dimensionalisation

We make the variables in equation (1) – (6) dimensionless by introducing the following dimensionless variables:

$$\left.\begin{array}{l}x'=\dfrac{x}{L},\ t'=\dfrac{Ut}{L},\ v'=\dfrac{v}{U},\ \psi_1=\dfrac{\varphi_s}{\varphi_{so}},\ \psi_2=\dfrac{\varphi_m}{\varphi_{mo}},\ \psi_3=\dfrac{\varphi_c}{\varphi_{co}},\ \phi=\dfrac{C_{ox}-C_{ox_\infty}}{C_{ox_o}-C_{ox_\infty}}\\ \in=\dfrac{RT_0}{E},\ \theta=\dfrac{E(T-T_o)}{RT_o^{\,2}},\ f=\dfrac{E_1}{E_3},\ r=\dfrac{E_2}{E_3}\end{array}\right\} \quad (7)$$

Where

x' is the dimensionless distance, t' is the dimensionless time, L is length in meters, U is the reference velocity, (ψ_1, ψ_2, ψ_3) are the dimensionless volume fractions of dry organic substance, moisture and coke respectively, ϕ is the dimensionless form of oxygen concentration, θ is the dimensionless form of temperature and $\in$ is the dimensionless activation energy.

Then equation (1)—(6) (after dropping prime) becomes;

$$\frac{\partial \psi_1}{\partial t} = -a\psi_1 e^{\frac{f\theta}{1+\in\theta}} \tag{8}$$

$$\frac{\partial \psi_2}{\partial t} = -b\psi_2 (1+\in\theta)^{\frac{1}{2}} e^{\frac{r\theta}{1+\in\theta}} \tag{9}$$

$$\frac{\partial \psi_3}{\partial t} = \beta\psi_1 e^{\frac{f\theta}{1+\in\theta}} - \gamma(\phi+q)\psi_3 e^{\frac{\theta}{1+\in\theta}} \tag{10}$$

$$\left.\begin{aligned} &\frac{\partial \phi}{\partial t} + v\frac{\partial \phi}{\partial x} = \frac{\partial}{\partial x}\left(D_1 \frac{\partial \phi}{\partial x}\right) - \beta_1\phi - \beta_2\psi_1(\phi+q)e^{\frac{f\theta}{1+\in\theta}} \\ &-\beta_3(1+\in\theta)^{\frac{1}{2}}\psi_2(\phi+q)e^{\frac{r\theta}{1+\in\theta}} - \beta_4\psi_3(\phi+p)(\phi+q)e^{\frac{\theta}{1+\in\theta}} \end{aligned}\right\} \tag{11}$$

$$\left.\begin{aligned} &\frac{\partial \theta}{\partial t} + v\frac{\partial \theta}{\partial x} = \frac{\partial}{\partial x}\left(\lambda_1 \frac{\partial \theta}{\partial x}\right) - \alpha_1(\theta+\gamma_1) - R_a(1+4\in\theta) - \delta\psi_2(1+\in\theta)^{\frac{1}{2}} e^{\frac{r\theta}{1+\in\theta}} \\ &+\delta_1\psi_3(\phi+q)e^{\frac{\theta}{1+\in\theta}} \end{aligned}\right\} \tag{12}$$

$$\left.\begin{aligned} &\psi_1(x,0)=1, \quad \psi_2(x,0)=1, \quad \psi_3(x,0)=1 \\ &\phi(x,0)=1, \quad \phi(0,t)=0, \quad \phi(1,t)=0 \\ &\theta(x,0)=0, \quad \theta(0,t)=\sigma_1, \quad \theta(1,t)=\sigma_1 \end{aligned}\right\} \tag{13}$$

where;

$$\left.\begin{aligned}
&a=\frac{k_1 L e^{\frac{-fE_1}{RT_o}}}{U},\quad b=\frac{k_2 T_o^{\frac{1}{2}} L e^{\frac{-rE_3}{RT_0}}}{U},\quad \beta=\frac{\alpha_c k_1 \rho_s \varphi_{so} L e^{\frac{-fE_3}{RT_0}}}{U\rho_c\varphi_{co}},\ \gamma=\frac{M_c k_3 S_\sigma \rho_g L}{M_1 U \rho_c}\left(C_{ox_o}-C_{ox_\infty}\right)e^{\frac{-E_3}{RT_o}},\\
&q=\frac{C_{ox_\infty}}{C_{ox_o}-C_{ox_\infty}},\quad D_1=\frac{D_T}{LU}=\frac{1}{P_{em}},\ \beta_1=\frac{\alpha L}{C_{pg}\Delta hU},\ \beta_2=\frac{\left(1-\alpha_c\right)k_1\rho_s\varphi_{so}L}{\rho_g U}e^{\frac{-fE_3}{RT_o}},\\
&\beta_3=\frac{k_2\rho_m T_o^{\frac{1}{2}}\varphi_{mo}Le^{\frac{-rE_3}{RT_o}}}{\rho_g U},\ \beta_4=\frac{k_3 S_\sigma \rho_g \frac{M_c}{M_1}\left[C_{ox_o}-C_{ox_\infty}\right]L\varphi_{co}e^{\frac{-E_3}{RT_o}}}{\rho_g U},\ p=\frac{\frac{M_1}{M_c}+C_{ox_\infty}}{C_{ox_o}-C_{ox_\infty}},\\
&\lambda_1=\frac{\lambda_T}{L\rho_g C_{pg}U}=\frac{1}{P_e},\quad \alpha_1=\frac{\alpha L}{\rho_g C_{pg}U},\ R_a=\frac{4K_R\sigma L T_o^{\,3}}{\rho_g C_{pg}\in U},\ \delta=\frac{k_2\rho_m q_2 T_o^{\frac{1}{2}}L\varphi_{mo}e^{\frac{-rE_3}{RT_o}}}{\rho_g C_{pg}\in T_o U},\\
&\delta_1=\frac{k_3 S_\sigma \rho_g q_3 \varphi_{co} L\left(C_{ox_o}-C_{ox_\infty}\right)}{\rho_g C_{pg}\in T_o U}e^{\frac{-E_3}{RT_o}},\ \gamma_1=\frac{T_o-T_\infty}{\in T_o},\quad \sigma_1=\frac{T_\infty-T_o}{\in T_o}
\end{aligned}\right\}\quad (14)$$

3.2 Approximate Analytical Solution

In this section, using perturbation method, we let

$$\left.\begin{aligned}
\psi_1&=\psi_{10}+\nu\psi_{11}+\ldots\\
\psi_2&=\psi_{20}+\nu\psi_{21}+\ldots\\
\psi_3&=\psi_{30}+\nu\psi_{31}+\ldots\\
\phi&=\phi_0+\nu\phi_1+\ldots\\
\theta&=\theta_0+\nu\theta_1+\ldots
\end{aligned}\right\}\quad (15)$$

Applying (15) in equations (8)—(13) and solving using direct integration and eigenfunction expansion technique given below;

$$\left.\begin{aligned}
&\frac{\partial u}{\partial t}=k\frac{\partial^2 u}{\partial x^2}+\alpha u+F\left(x,t\right)\\
&u\left(x,0\right)=f\left(x\right),\quad u\left(0,t\right)=0,\quad u\left(L,t\right)=0
\end{aligned}\right\}\quad (16)$$

We assume

$$u\left(x,t\right)=\sum_{n=1}^{\infty}u_n\left(t\right)\sin\frac{n\pi}{L}x \quad (17)$$

Where;

$$u_n(t)=\int_0^t e^{\left(\alpha-k\left(\frac{n\pi}{L}\right)^2\right)(t-\tau)}F_n(\tau)d\tau+b_n e^{\left(\alpha-k\left(\frac{n\pi}{L}\right)^2\right)t} \tag{18}$$

$$F_n(t)=\frac{2}{L}\int_0^L F(x,\mathrm{t})\sin\frac{n\pi}{L}xdx \tag{19}$$

$$b_n=\frac{2}{L}\int_0^L f(x)\sin\frac{n\pi}{L}xdx \tag{20}$$

we obtain analytical solution of the dimensionless equations (8)—(13) as follows:

$$\psi_1(x,t)=1+v\left(-A_3\sum_{n=1}^{\infty}A_2\sin n\pi x-a_6\left(t+\left(\begin{array}{l}f(e-2).\\\left(\sigma_1 t+\sum_{n=1}^{\infty}\left(A_1t-A_2e^{-c_2t}\right)\sin n\pi x\right)\end{array}\right)\right)\right) \tag{21}$$

$$\psi_2(x,t)=1+v\left(\begin{array}{l}-a_7\left(\begin{array}{l}t+r(e-2)\left(\sigma_1 t+\sum_{n=1}^{\infty}\left(A_1t-A_2e^{-c_2t}\right)\sin n\pi x\right)+\\\frac{1}{2}\in\left(\sigma_1 t+\sum_{n=1}^{\infty}\left(A_1t-A_2e^{-c_2t}\right)\sin n\pi x\right)+\\\frac{1}{2}\in\left(r(e-2)\right)\left(\begin{array}{l}\sigma^2{}_1t+2\sigma_1\left(\sum_{n=1}^{\infty}\left(A_1t-A_2e^{-c_2t}\right)\sin n\pi x\right)\\+\sum_{n=1}^{\infty}\sum_{n=1}^{\infty}\left(\begin{array}{l}A_1{}^2t-\frac{2A_1}{c_2}(b_n-A_1)e^{-c_2t}\\-\frac{(b_n-A_1)^2}{2c_2}e^{-2c_2t}\end{array}\right)\sin^2 n\pi x\end{array}\right)\end{array}\right)\\-a_7\left(A_7+\sum_{n=1}^{\infty}B_1\sin n\pi x\right)\sum_{n=1}^{\infty}A_2\sin n\pi x\end{array}\right) \tag{22}$$

$$\psi_3(x,t)=1+v\left(\begin{array}{l}a_9\left(A_8t+A_9\sum_{n=1}^{\infty}\left(A_1t-A_2e^{-c_2t}\right)\sin n\pi x\right)\\+a_8\left(\begin{array}{l}A_{10}\sum_{n=1}^{\infty}\frac{A}{c_1}e^{-c_1t}\sin n\pi x+A_{11}\sum_{n=1}^{\infty}\sum_{n=1}^{\infty}\left(B_2e^{-c_1t}+B_3e^{-(c_1+c_2)t}\right)\sin^2 n\pi x\\-A_{12}t-A_{13}\sum_{n=1}^{\infty}\left(A_1t-A_2e^{-c_2t}\right)\sin n\pi x\end{array}\right)\\+a_9A_9\sum_{n=1}^{\infty}A_2\sin n\pi x-a_8\left(\begin{array}{l}A_{10}\sum_{n=1}^{\infty}\frac{A}{c_1}\sin n\pi x+A_{11}\sum_{n=1}^{\infty}\sum_{n=1}^{\infty}(B_4)\sin^2 n\pi x\\+A_{13}\sum_{n=1}^{\infty}A_2\sin n\pi x\end{array}\right)\end{array}\right) \tag{23}$$

$$\phi(x,t)=\sum_{n=1}^{\infty}Ae^{-c_1t}\sin n\pi x+v\left(\sum_{n=1}^{\infty}\left(\begin{array}{l}-2A_{49}\sum_{n=1}^{\infty}Ate^{-c_1t}-2A_{50}\sum_{n=1}^{\infty}\left[\frac{A_1}{c_1}+A_{53}e^{-c_2t}-A_{54}e^{-c_1t}\right]\\ -A_{56}\left[1-e^{-c_1t}\right]-2A_{51}\sum_{n=1}^{\infty}\sum_{n=1}^{\infty}A_{52}\left[\begin{array}{l}AA_1te^{-c_1t}-A_{55}e^{-(c_1+c_2)t}\\ +A_{55}e^{-c_1t}\end{array}\right]\\ -2A_{42}\sum_{n=1}^{\infty}\sum_{n=1}^{\infty}A_{52}\left[\begin{array}{l}\frac{A_1^2}{c_1}+A_{57}e^{-c_2t}+A_{58}e^{-2c_2t}-\frac{A_1^2}{c_1}e^{-c_1t}\\ -A_{57}e^{-c_1t}-A_{58}e^{-c_1t}\end{array}\right]\\ -2A_{43}\sum_{n=1}^{\infty}\sum_{n=1}^{\infty}\sum_{n=1}^{\infty}\left[\begin{array}{l}AA^2{}_1te^{-c_1t}-A_{59}e^{-(c_1+c_2)t}\\ -A_{59}e^{-(c_1+c_2)t}-A_{60}e^{-(c_1+2c_2)t}\\ +A_{59}e^{-c_1t}+A_{59}e^{-c_1t}+A_{60}e^{-c_1t}\end{array}\right]\\ +2A_{44}\sum_{n=1}^{3}\sum_{n=1}^{3}A_{61}\left[1-e^{-c_1t}\right]-2A_{45}\sum_{n=1}^{\infty}\sum_{n=1}^{\infty}A_{52}\left[\begin{array}{l}AA_1te^{-c_1t}\\ -A_{55}e^{-(c_1+c_2)t}\\ +A_{55}e^{-c_1t}\end{array}\right]\\ +2A_{46}\sum_{n=1}^{\infty}\sum_{n=1}^{\infty}\sum_{n=1}^{\infty}\left[A_{62}e^{-2c_1t}+A_{63}e^{-(2c_1+c_2)t}-A_{62}e^{-c_1t}-A_{63}e^{-c_1t}\right]\end{array}\right)\sin n\pi x \qquad (24)$$

$$\theta(x,t)=\left(\sigma_1+\sum_{n=1}^{\infty}\left(A_1+\left(b_n-A_1\right)e^{-c_2t}\right)\sin n\pi x\right)+$$
$$v\left(\sum_{n=1}^{\infty}\left(\begin{array}{l}-2\frac{A_{72}}{c_2}\left[1-e^{-c_2t}\right]-2A_{73}\sum_{n=1}^{\infty}\left[\frac{A_1}{c_2}+\left(b_n-A_1\right)te^{-c_2t}-\frac{A_1}{c_2}e^{-c_2t}\right]\\ -2A_{68}\sum_{n=1}^{\infty}\sum_{n=1}^{\infty}A_{52}\left[\begin{array}{l}\left[1-e^{-c_2t}\right]\frac{A_1^2}{c_2}+2A_1\left(b_n-A_1\right)te^{-c_2t}\\ +\left[e^{-c_2t}-1\right]\frac{\left(b_n-A_1\right)^2}{c_2}\end{array}\right]\\ +2A_{69}\sum_{n=1}^{\infty}\frac{A}{\left(c_2-c_1\right)}\left[e^{-c_1t}-e^{-c_2t}\right]+2A_{70}\sum_{n=1}^{\infty}\sum_{n=1}^{\infty}A_{52}\left[\begin{array}{l}\frac{AA_1}{\left(c_2-c_1\right)}e^{-c_1t}-\frac{A\left(b_n-A_1\right)}{c_1}e^{-(c_2+c_1)t}\\ -\frac{AA_1}{\left(c_2-c_1\right)}e^{-c_2t}+\frac{A\left(b_n-A_1\right)}{c_1}e^{-c_2t}\end{array}\right]\end{array}\right)\sin n\pi x\right) \qquad (25)$$

where;

$$c_1=\left(\beta_1+D_1\left(n\pi\right)^2\right),\ A=\frac{2\left[1-\left(-1\right)^n\right]}{n\pi},\ b_1=\left(4R_a\in+\alpha_1\right),\ b_2=\left(\sigma_1\left(4R_a\in+\alpha_1\right)+\left(R_a+\alpha_1\gamma_1\right)\right),$$

$$c_2=\left(b_1+\lambda_1\left(n\pi\right)^2\right),\ A_1=\frac{2b_2\left[\left(-1\right)^n-1\right]}{n\pi c_2},\ A_2=\left(\frac{b_n-A_1}{c_2}\right),\ A_3=a_6f\left(e-2\right),\ A_4=r\left(e-2\right),$$

$$A_5=\frac{1}{2}\in,\ A_6=\in\left(r\left(e-2\right)\right)\sigma_1,\ B=\frac{b_n-A_1}{2},\ B_1=\left(2A_1+B\right),\ A_7=\left(A_4+A_5+A_6\right),\ b_n=\frac{2\sigma_1}{n\pi}\left[\left(-1\right)^n-1\right]$$

$$A_8=\left(1+f\left(e-2\right)\sigma_1\right),\ A_9=f\left(e-2\right),\ A_{10}=\left(1+\left(e-2\right)\sigma_1\right),\ A_{11}=\left(e-2\right),\ B_2=\frac{AA_1}{c_1},$$

$$B_3=\frac{A\left(b_n-A_1\right)_1}{c_1+c_2},\ A_{12}=\left(1+\left(e-2\right)\sigma_1\right)q,\ A_{13}=\left(e-2\right)q,\ B_4=\left(B_2+B_3\right),\ A_{14}=\left(1+f\left(e-2\right)\sigma_1\right)q,$$

$$A_{15}=f\left(e-2\right)q,\ A_{16}=\left(1+r\left(e-2\right)\sigma_1\right),\ A_{17}=r\left(e-2\right),\ A_{18}=\left(1+r\left(e-2\right)\sigma_1\right)q,A_{19}=r\left(e-2\right)q,$$

$$A_{20}=\frac{1}{2}\in\left(\left(1+r\left(e-2\right)\sigma_1\right)\sigma_1\right),\ A_{21}=\frac{1}{2}\in r\left(e-2\right)\sigma_1,\ A_{22}=\frac{1}{2}\in\left(\left(1+r\left(e-2\right)\sigma_1\right)\sigma_1q\right),$$

$$A_{23}=\frac{1}{2}\in r\left(e-2\right)\sigma_1q,\ A_{24}=\frac{1}{2}\in\left(1+r\left(e-2\right)\sigma_1\right),\ A_{25}=\frac{1}{2}\in r\left(e-2\right),\ A_{26}=\frac{1}{2}\in\left(1+r\left(e-2\right)\sigma_1\right)q,$$

$$A_{27}=\frac{1}{2}\in r\left(e-2\right)q,\ A_{28}=\left(p+q\right)\left(1+\left(e-2\right)\sigma_1\right),\ A_{29}=\left(p+q\right)\left(e-2\right),\ A_{30}=\left(pq\right)\left(1+\left(e-2\right)\sigma_1\right),$$

$$A_{31}=\left(pq\right)\left(e-2\right),A_{32}=\left(a_1A_{14}+a_2A_{18}+a_2A_{22}+a_3A_{30}\right),\ A_{33}=\left(a_1A_{16}+a_2A_{20}\right),\ A_{34}=\left(a_2A_{19}+a_2A_{23}+a_2A_{26}\right),$$

$$A_{35}=\left(a_2A_{17}+a_2A_{21}+a_2A_{22}+a_2A_{24}\right),\ A_{36}=\frac{1}{2}a_1A_8,\ A_{37}=\frac{1}{2}a_1A_{15},\ A_{38}=\frac{2}{3}a_1A_9,\ A_{39}=\frac{1}{2}A_{33},\ A_{40}=\frac{1}{2}A_{34},$$

$$A_{41}=\frac{2}{3}A_{35},\ A_{42}=\frac{2}{3}a_2A_{27},\ A_{43}=\frac{3}{8}a_2A_{25},\ A_{44}=\frac{2}{3}a_3A_{10},\ A_{45}=\frac{2}{3}a_3A_{29},\ A_{46}=\frac{3}{8}a_3A_{11},\ A_{47}=\frac{1}{2}a_3A_{38},$$

$$A_{48}=\frac{1}{2}a_3A_{31},\ A_{49}=\left(A_{36}+A_{39}+A_{47}\right),\ A_{50}=\left(A_{37}+A_{40}+A_{48}\right),\ A_{51}=\left(A_{38}+A_{41}\right),\ A_{52}=\left[\frac{1-\left(-1\right)^n}{n\pi}\right],$$

$$A_{53}=\frac{b_n-A_1}{c_1-c_2},\ A_{54}=\frac{A_1\left(c_1-c_2\right)+c_1\left(b_n-A_1\right)}{c_1\left(c_1-c_2\right)},\ A_{55}=\frac{A\left(b_n-A_1\right)}{c_2},\ A_{56}=2\frac{A_{32}A_{52}}{c_1},\ A_{57}=\frac{2A_1\left(b_n-A_1\right)}{c_1-c_2},$$

$$A_{58}=\frac{\left(b_n-A_1\right)^2}{\left(c_1-2c_2\right)},\ A_{59}=\frac{AA_1\left(b_n-A_1\right)}{c_2},\ A_{60}=\frac{A\left(b_n-A_1\right)^2}{2c_2},\ A_{61}=\frac{A_{52}A^2}{c_1},\ A_{62}=\frac{A^2A_1}{c_1},\ A_{63}=\frac{A^2\left(b_n-A_1\right)}{\left(c_1+c_2\right)},$$

$$A_{64}=\left(a_4A_{16}+a_4A_{20}-a_5A_{12}\right),\ A_{65}=\frac{a_4A_{17}}{2},\ A_{66}=\frac{a_4A_{21}}{2},\ A_{67}=\frac{a_4A_{24}}{2},\ A_{68}=\frac{2a_4A_{25}}{3},\ A_{69}=\frac{a_5A_{10}}{2},$$

$$A_{70}=\frac{2a_5A_{11}}{3},\ A_{71}=\frac{a_5A_{13}}{2},\ A_{72}=\left(A_{64}A_{52}\right),\ A_{73}=\left(A_{65}+A_{66}+A_{67}-A_{71}\right)$$

The computation were done using computer symbolic algebraic package MAPLE to generate the graphs.

RESULTS AND DISCUSSION

We analysed the effect Radiation number (R_a), Peclet energy number (P_e), Peclet mass number (P_{em}) and Equilibrium wind velocity (v) on oxygen concentration $\phi(x,t)$. Analytical solution given by equation (15)—(19), is computed using computer symbolic algebraic package MAPLE 17. The numerical results obtained from the method are shown in Figures 1, 2, 3 and 4.

Figure 1 displays the graph of oxygen concentration $\phi(x,t)$ against distance x and time t for different values of Radiation number (R_a). It is observed that the oxygen concentration oscillates along the distance and does not change with time but the maximum concentration decreases as the Radiation number increases.

Figure 2 depicts the graph of oxygen concentration $\phi(x,t)$ against distance x for different values of Peclet energy number (P_e). It is observed that the oxygen concentration oscillates along the distance and maximum concentration decreases as the Peclet energy number increases.

Figure 3 depicts the graph of oxygen concentration $\phi(x,t)$ against distance x for different values of Peclet mass number (P_{em}). It is observed that the oxygen concentration oscillates along the distance and maximum concentration increases as the Peclet mass number increases.

Figure 4 depicts the graph of oxygen concentration $\phi(x,t)$ against distance x for different values of equilibrium wind velocity (v). It is observed that the oxygen concentration oscillates along the distance and maximum concentration increases as the equilibrium wind velocity increases.

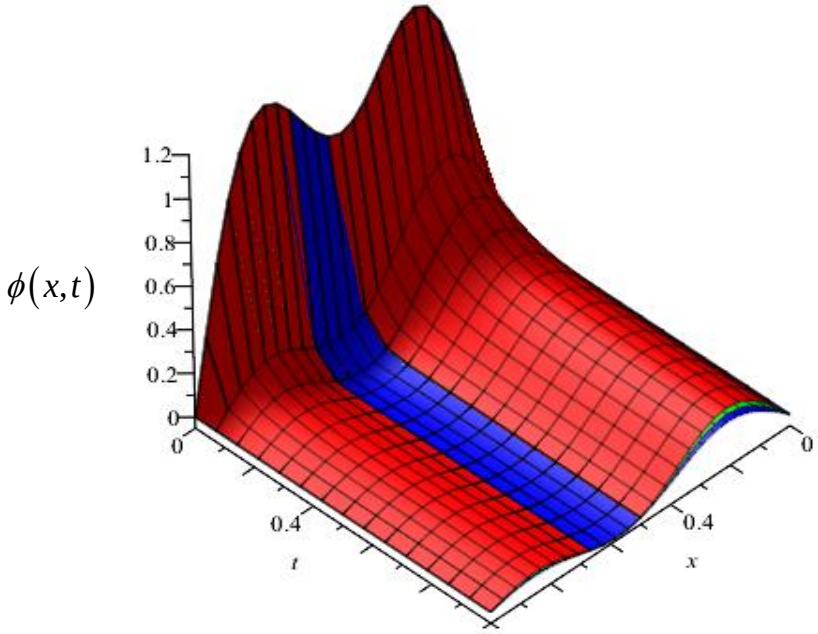

Figure 1: Effect of Radiation number (R_a) on oxygen concentration

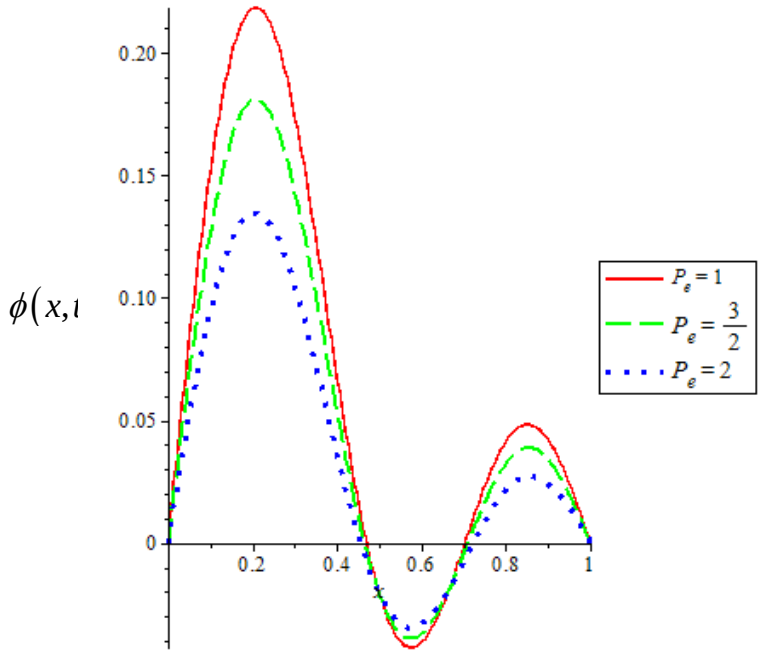

Figure 2: Effect of Peclet energy number (P_e) on oxygen concentration

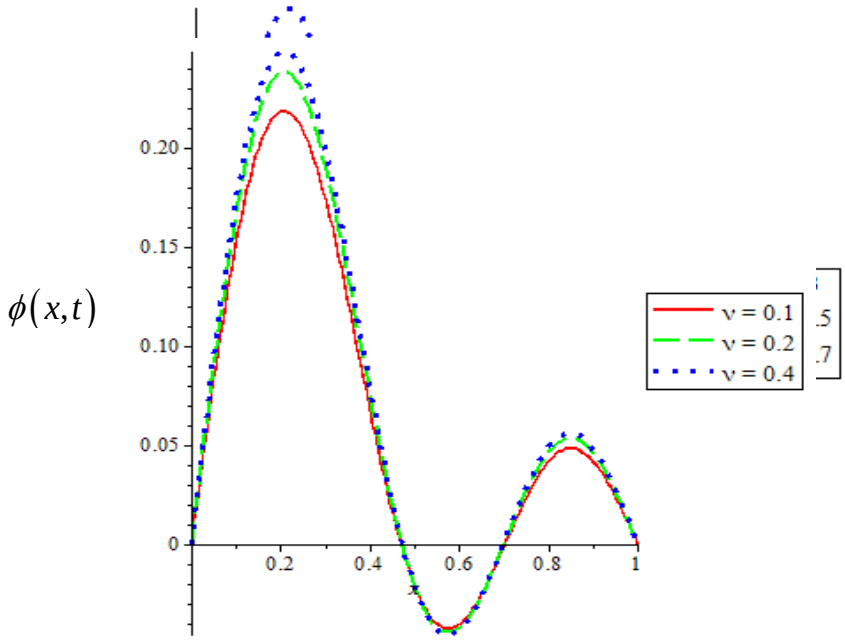

Figure 3: Effect of Peclet mass number (P_{em}) on oxygen concentration

Figure 3: Effect of Equilibrium wind velocity (v) on oxygen concentration

It is observed that increase in the radiation and peclect energy number results in depreciation of oxygen concentration, while increase in peclet mass number and equilibrium wind velocity enhanced maximum oxygen concentration as demonstrated in Figures 1, 2, 3 and 4 respectively. Therefore, it is important for fire fighters to take into account the effects of these parameters as it influences oxygen concentration.

CONCLUSION

From the studies made on this paper, we conclude that as radiation and peclect energy number gained increase, oxygen concentration decelerates and accelerates as peclet mass number and equilibrium wind velocity increases. The inference drew from this analysis wholly deals with concentration profile that stimulate the rate at which wind affect fire outbreak. The aim of any fire fighter is to supress the level of fire spread. Therefore, with continuous increase in radiation and peclet energy number we see that the level of oxygen concentration is retard which reduces the escalation of fire spread.

The results may be used as a preliminary predictive tool to study mathematically the forward propagation of fire outbreak in coupled atmospheric-wildfire.

REFERENCES

Freitas, S. R., Longo, K. M., Silva-Dias, M. A. F., Silva-Dias, P. L., Chatfield, R., Prins, E., Artaxo, P., Grell, G. A., & Recuero, F. S. (2005). Monitoring the transport of biomass burning emissions in South America. *Environ. Fluid Mech. 5, 135–167.*

Mandel, J., Jonathan, D. B., & Adam, K. K. (2018). Coupled atmosphere-wildland fire modelling with WRF-Fire version 3.3

Meroney, R. N. (2007). Fires in porous media: Natural and urban canopies. In: Gayev, Y.A., and Hunt, J.C.R. eds. Flow and Transport Processes with Complex Obstructions, 271–310. Springer, Netherlands.

Perminov, V. A. (2018). Mathematical modelling of wildland fires initiation and spread using a coupled atmospheric-forest fire setting, *The Italian Association of Chemical Engineering, 70, 1747-1752* doi: 10.3303/CET1870292 ISBN978-88-95608-67-9; ISSN 2283-9216

Potter, B. E. (2002). A dynamics based view of atmosphere–fire interactions. *International Journal of Wildland Fire 11, 247–255.*

Randall, P. B., John, O. R., & David, R. W. (2009). Climatic and Weather Factors Affecting Fire Occurrence and behavior. *Developments in Environmental Science, Volume 8.* ISSN: 1474-8177/DOI:10.1016/S1474-8177(08)00002-8.

Taylor, S. W., Wotton, B. M., Alexander, M. E., & Dalrymple, G. N. (2004). Variation in wind and crown fire behaviour in a northern jack pine—black spruce forest. *Can. J. For. Res. 34, 1561–1576.*

Zhiri, A. B., Olayiwola, R. O. & Odo, C. E. (2020). Modeling fire spread behavior in coupled atmospheric-forest fire. *Journal of Science, Technology, Mathematics and Education (JOSTMED), 16(4), pp 104-113*